Military Technical College
Kobry El-kobbah,
Cairo, Egypt

5th International Conference
on Electrical Engineering
ICEENG 2006

PERFORMANCE IMPROVEMENT OF THERMAL IMAGES

Gouda Ismail Salama*, Mohamed El-Said Ghoneimy*,
Wael Mohamed Yousf*

Abstract

This paper describes and evaluates a number of techniques for reducing different types of noises which associated with the thermal images. These techniques are based on optical image filtering in both spatial domain and frequency domain. Filtering in both spatial domain and frequency domain are applied on different thermal images associated with three standard noises models encountered in most images as additive, multiplicative, and impulse noises with different variance. Also, Non-uniformity correction techniques are applied on several thermal images associated with Fixed Pattern Noise (FPN). The algorithms have been tested by using several real image data from existing infrared imaging systems with good results. Measuring criteria for performance evaluation of thermal images enhancement techniques as Peak Signal-to-Noise Ratio (PSNR), Signal-to-Noise Ratio (SNR) and Root Mean Square Error (RMSE) are used to ensure the vision observation of user to select the most suitable technique with highly performance evaluation.

Keyword: Thermal imagery, Image enhancement, Filtering, non-uniformity correction, performance evaluation.

1- Introduction

The performance of any image processing system depends on the quality of the input images, which makes image enhancement and pre-processing an important field of research. Compensating for non linear optical sensors, enhancing or suppressing different parts of the image and reducing noise distortion are examples of common image pre-processing. This paper concerns the latter.

All image sensors, consists of an array of detector elements, suffer from an undesired effect, spatial non-uniformity among the array elements of image sensor. Called fixed pattern noise (FPN) [1] [2]. It is mainly due to variations in detector dimensions, doping concentrations, contamination during fabrication. Due to the existence of some nature components as CO_2 and H_2O that absorbs amount of heat emitted from object, besides the dust in the air that making scattering process which leads to decrease in signal intensity at the edges of the image and different kinds of circular image artifacts.

In the past two decades, various techniques have been proposed and used to remedy this non-uniformity problem. The most basic and effective solution for correcting non-uniformity is the radiometric calibration of the camera, where the camera is exposed to one or more spatially-constant and known irradiation sources. The calibration process can be as simple as dropping a constant-temperature shutter in front of the camera's field-of-view (FOV), or it could involve the use of a black-body source, operated at multiple temperatures. Although

calibration is generally a good solution to the non-uniformity problem, it is undesirable for several reasons. First, one needs to perform the calibration as frequently as needed, which is dictated by the speed at which the non-uniformity drifts over time. Second, good calibration often requires the use of one or more black-body sources, which are expensive and require their own electrical and mechanical hardware for their control and interface with the camera.

As a result of the often complex and always disruptive nature of calibration, techniques that achieve non-uniformity correction by means of post-processing are highly motivating and attractive in many applications. These techniques are often referred to as "scene-based" non-uniformity correction (NUC) techniques, since they do not require imaging special scenes obtained from the calibration source for the purpose of calibration. Two main categories of post-processing NUC techniques have been developed: (1) statistical techniques and (2) algebraic techniques. The statistical techniques model the FPN as a random spatial noise and estimate the statistics of the noise to remove it. The algebraic techniques, on the other hand, make use of global motion between the frame in the video sequence and attempt to compensate for the non-uniformity by means of algebraic methods without making statistical assumptions about the FPN [3].

Also there are three standard noise models which model well the types of noise encountered in most images: additive, multiplicative, and impulse noise [4]. These noises are produced by numerous factors including thermal effects, sensor saturation, quantization errors and transmission errors.

Section 2 present several types of noises associated with thermal images. Section 3 introduces the measuring criteria for performance evaluation of thermal images enhancement techniques. Section 4 introduces a study analysis on some of enhancement techniques. Section 5 shows the analysis that is performed on the most popular enhancement techniques, and comparative study between these techniques. Section 6 concludes the work result. Finally, references are given in section 7.

2- Noise models

This section reports the three standard noises models encountered in most images as the additive, multiplicative, and impulse. Also, it discuss the fixed pattern noise which is the main dominant noise associated with the thermal images.

2.1. Additive noise

Let $f'(x,y)$ be the noisy digitized version of the ideal image, $f(x,y)$ and $n(x,y)$ be a "noise function" which returns random values coming from an arbitrary distribution. The additive Noise generally represented as a normally distributed (Gaussian), zero-mean random process with a probability density function by equation (1):

$$n(x,y) = \frac{1}{\sqrt{2\pi\sigma_n}} \ell^{-\frac{(x^2+y^2)}{2{\sigma_n}^2}} \quad (1)$$

$$f'(x,y) = f(x,y) + n(x,y) \quad (2)$$

Additive noise is independent of the pixel values in the original image. Typically, $n(x,y)$ is symmetric about zero. Additive noise is a good model for the thermal noise within Photo-electronic sensors [5].

2.2 Multiplicative noise

Multiplicative noise, or speckle noise, is a signal dependent form of noise whose magnitude is related to the value of the original pixel. Equation (3) describes one simple form it can take, but a more complex function of the original pixel value is also possible.

$$f'(x,y) = f(x,y) + n(x,y)\ \ f(x,y) \tag{3}$$

$$n(x,y) = \frac{1}{\sqrt{2\pi\sigma_n}}\,\ell^{-\frac{((x-1)^2+(y-1)^2)}{2\sigma_n^2}} \tag{4}$$

2.3 Impulse noise

Impulse noise has the property of either leaving a pixel unmodified with probability 1-p, or replacing it altogether with probability p. This is shown in equation (5) Restricting $n(x,y)$ to producing only the extreme intensities 0 or Z-1 results in *salt-pepper* noise [6] [7].

$$f'(x,y) = \begin{cases} n(x,y) \rightarrow probability(p) \\ f(x,y) \rightarrow prob.(1-p) \end{cases} \tag{5}$$

2.4 Fixed pattern noise (FPN)

Is the spatial variation in pixel output values under uniform illumination due to device and interconnect parameter variations (mismatches) across the sensor [3]. The most common FPN sources include fabrication errors, cooling system, electronics, and optics.

3- Measuring criteria for performance evaluation

The enhanced image quality could be measured using the root mean square error (RMSE), Signal to noise ratio (SNR), and Peak signal to noise ratio (PSNR).

RMSE is the square root of the mean square error between the original and enhanced image. It detects the difference between the enhanced and the original image [8].

$$\text{RMSE} = \sqrt{\frac{1}{M \times N}\sum_{x=0}^{M-1}\sum_{y=0}^{N-1}(g(x,\ y) - f(x,\ y))^2} \tag{6}$$

Where:

f(x,y)…….. The original or input image.
g(x,y)……. The output image (the enhanced image after enhancement process).
M × N …. The image size.

SNR relates the mean square error to the enhanced image energy

$$\text{SNR} = 10\log\left[\frac{\sum_{x=0}^{M-1}\sum_{y=0}^{N-1} g^2(x,y)}{\sum_{x=0}^{M-1}\sum_{y=0}^{N-1}(g(x,y) - f(x,y))^2}\right] \quad [\text{dB}] \tag{7}$$

PSNR is defined as [8]:

$$\text{PSNR} = 10\log\left[\frac{X_{max}^2}{\frac{1}{MxN}\sum_{x=0}^{M-1}\sum_{y=0}^{N-1}(g(x,y) - f(x,y))^2}\right] \quad [\text{dB}] \tag{8}$$

Where, X_{max} is the maximum gray level (255 for 8-bit level) of the given input image.

4- Performance improvement of thermal images

The principle objective of image enhancement is to improve the quality of thermal images, in other word enhancement is to process an image so that the result is more suitable than the original image for a specific application. Image enhancement approaches fall into two board categories: spatial domain methods and frequency domain methods. The term spatial domain refers to the image plane itself, and techniques in this category are based on direct manipulation of pixels in an image. Frequency domain processing techniques are based on modifying the Fourier transform of an image.

4.1. Image enhancement in the spatial domain

Spatial filtering process consists simply of moving the filter mask from point to point in an image. At each point (x, y) the response of the filter at that point is calculated using a predefined relationship. In general, linear filtering of an image f of size $M \times N$ with a filter mask of size $m \times n$ is given by [9]

$$g(x,y) = \sum_{s=-a}^{a} \sum_{t=-b}^{b} w(s,t) f(x+s, y+t) \qquad (9)$$

Where

a= (m -1)/2 and b= (n -1)/2

To generate a complete filtered image this equation must be applied for

x =0, 1, 2… M-1

y = 0, 1, 2… N-1

In this paper we concerned with median and circular average filters.

4.2. Image enhancement in the frequency domain

The basic "model" for filtering in the frequency domain is given by

$$G(u,v) = H(u,v)\, F(u,v) \qquad (8)$$

Where

$G(u,v)$ The Fourier transform of the output image

$F(u,v)$ The Fourier transform of the input image

$H(u,v)$ The filter transfer function

In this paper we concerned with ideal low-pass filter, Butter worth low-pass filter, Gaussian low-pass filter and wiener filters. These filters cover the range from very sharp (ideal) to very smooth filter functions [9].

4.3. Non-uniformity correction

Though imaging systems with reference-based non-uniformity correction are accurate, they often involve opt-mechanic components and temperature references that are expensive and complex in design. To overcome this problem, a lot of research has been focused on performing sensor calibration entirely in software. Methods have been presented here: scene-based non-uniformity correction and One-image correction [10].

4.3.1. Scene-based non-uniformity correction

scene-based non-uniformity correction (Temporal highpass filter) applied on a sequence of infrared image data consist of scene information, varying from frame to frame, and a fixed pattern noise, roughly the same in all frames. This means that when studying each pixel individually over time, high-frequency information belongs to the scene, while low-frequency

information belongs to fixed pattern noise. An estimate of the noise is thus obtained by lowpass filtering the image sequence along the temporal axis. When subtracting this estimate from an input image frame, non-uniformity correction is performed. The whole process acts like a temporal highpass filter that given by [9]

$$H(u,v) = \frac{1}{1+\left[D_0 / D(u,v)\right]^{2n}} \qquad (9)$$

Where

D_0 is a specified nonnegative quantity, and $D(u,v)$ the distance from point (u,v) to the origin of the frequency Rectangle.

4.3.2. One-image correction

Usually, some properties and characteristics of the fixed pattern noise is known in advance. For example, pixel intensity is generally lower at the edges of the image, and pixel-to-pixel correlation is visible as grid and line patterns. This knowledge can be used to produce an estimate of the fixed pattern noise as an initial set of correction parameters for further processing by the non-uniformity correction algorithms. It seems that every second pixel is somewhat correlated. This is also evident when examining the Fourier transform of the image. Once identified, these frequency components may be filtered out to remove most of the grid noise, the grid noise is mostly additive in origin, while the pixel intensity decrease at the image edges is part of a slowly varying multiplicative fixed pattern noise. By taking the logarithm of the image, this noise will be turned into additive noise, which then can be reduced by applying a high pass filter. This is sometimes referred to as homomorph filtering [9][10] given by

$$H(u,v) = (\gamma_H - \gamma_L)[1 - e^{-c(D^2(u,v)/D_O{}^2}] + \gamma_L \qquad (10)$$

Where

c is constant to control the sharpness of the filter function,

γ_H and γ_L are chosen parameter so that γ_L <1 and γ_H >1.

5- Experimental work

The applied algorithms were tested using samples of 8-bits thermal images of different sizes (see fig.1). The three standard noises were artificially added in these images at various noise ratios. The performances of the applied algorithms are evaluated using PSNR in different cases.

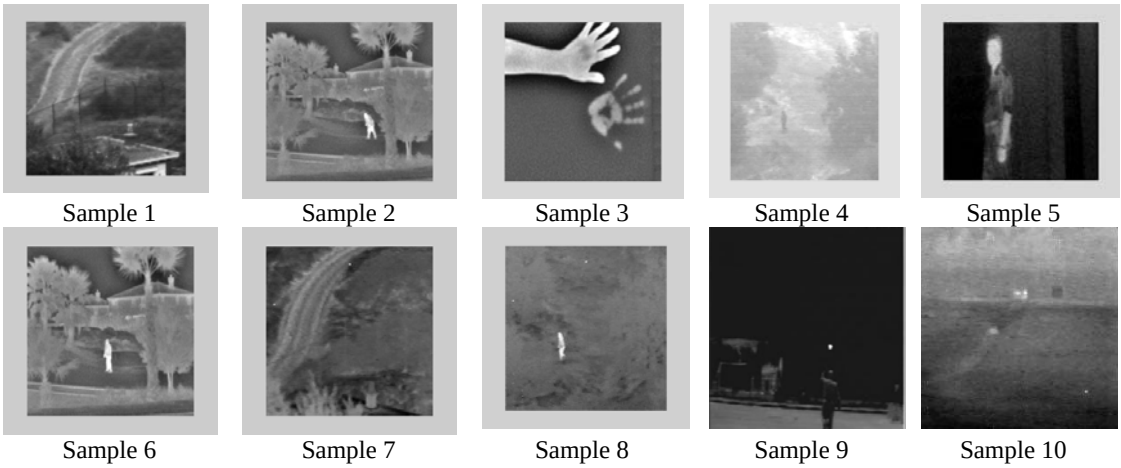

Fig.1. Examples of thermal images

The first Experiment is conducted to gauge the efficiency of the applied technique for filtering images corrupted at different noise ratio. The result of sample image is shown in Figure (2), where the noise ratios for impulses noise range from 2.5% to 50%. It is seen visually from these graphical figures that non linear filter represented in median filter provides superior results to the other filters in reducing impulse noises (with non linear behavior) at different noise density values.

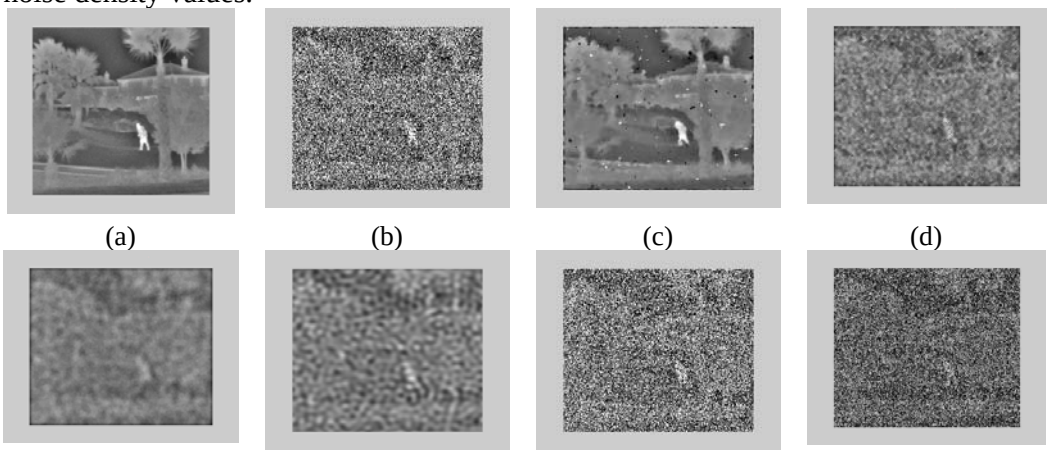

(a) (b) (c) (d)

(e) (f) (g) (h)

Fig.2. An example of thermal images corrupted by salt & pepper with noise density 50% after applying different filters for noise reduction.(a) Original image, (b) image corrupted with Salt & pepper noise, (c) applying Median filter, (d) applying Wiener filter, (e) applying circular averaging filter, (f) applying ILP filter, (g) applying BLP filter, (h) applying GLP filter.

To assess the effectiveness of the implemented filters in processing different thermal images. Tables [1, 2, and 3] present the comparison results for images degraded by impulse noises. It is seen from these tables that PSNR values of the median filter has the largest value compared with other filters. So, the median filter is the most suitable filter for reducing the impulse noise hence it replaces the value of a pixel by the median of the gray levels in the neighborhood of that pixel. Median filters provide excellent noise reduction capabilities, with considerably less blurring than linear spatial filter of similar size.

Table 1. Comparative results in PSNR (dB) of filtering ten different thermal images corrupted by 50% impulses noise.

filters	median	wiener	Circular average	ILPF	BLPF	GLPF
Img.1	24.10	18.44	18.17	8.47	9.27	9.50
Img.2	23.09	18.25	18.03	8.28	9.99	10.08
Img.3	22.46	20.57	20.23	8.61	10.18	9.93
Img.4	22.26	17.51	17.33	8.63	10.21	10.23
Img.5	20.64	18.24	17.75	8.75	10.19	10.42
Img.6	23.87	13.67	13.64	8.47	10.31	10
Img.7	22.26	20.35	20.16	8.43	10.11	10.02
Img.8	23.46	18.59	18.41	9.24	12.67	11.64
Img.9	23.64	21.17	20.44	8.83	10.97	10.30
Img.10	20.54	17.43	17.39	8.76	10.76	9.98

average	22.63	18.42	18.15	8.57	10.18	10.20

Table 2. Comparative results in PSNR (dB) of filtering ten different thermal images corrupted by 5% impulses noise.

filters	median	wiener	Circular average	ILPF	BLPF	GLPF
Img.1	31.21	23.76	24.91	18.49	19.24	19.45
Img.2	37.66	23.64	26.75	18.22	20.34	19.89
Img.3	38.42	24.79	26.51	18.35	20.19	18.84
Img.4	37.44	24.42	26.95	18.23	20.54	19.87
Img.5	37.50	24.75	27.28	18.83	20.12	19.76
Img.6	38.58	24.34	26.05	18.65	20.23	18.69
Img.7	38.07	24.42	26.04	18.41	20.47	18.87
Img.8	26.37	22.23	23.40	19.34	21.46	20.16
Img.9	34.38	22.55	25.10	18.73	21.98	19.92
Img.10	34.60	22.79	25.46	18.73	20.85	20.01
average	35.42	23.76	25.84	18.59	20.54	19.54

Table 3. Comparative results in PSNR (dB) of filtering ten different thermal images corrupted by 2.5% impulses noise.

filters	median	wiener	Circular average	ILPF	BLPF	GLPF
Img.1	39.14	25.87	29.21	22.16	22.65	24.92
Img.2	37.81	24.95	28.97	21.39	22.83	22.45
Img.3	40.98	26.06	28.38	21.41	21.68	25.01
Img.4	38.01	25.58	29.07	21.67	22.38	26.81
Img.5	38.15	25.91	29.47	21.28	22.41	26.92
Img.6	40.84	25.60	28.02	21.27	22.43	21.43
Img.7	39.54	26.13	27.97	21.55	23.67	20.99
Img.8	26.57	23.41	24.39	22.56	22.16	22.16
Img.9	35.17	23.99	27.34	22.17	22.35	21.35
Img.10	35.11	24.22	28.44	21.92	22.89	21.67
average	37.13	25.17	28.12	21.73	22.54	23.37

Figure 3, showing the performance comparison of different filters with different density of noises. It can be shown that PSNR at different values of impulse noise densities that, median filter has large value comparative with other filters.

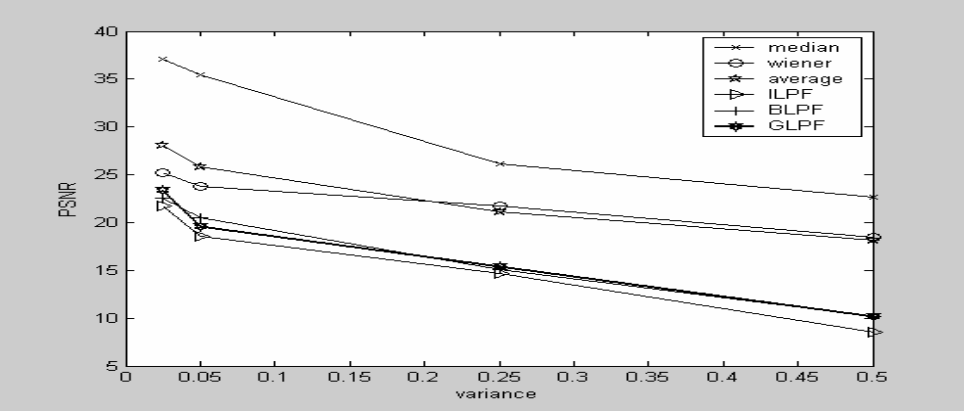

Fig.3. Performance comparison of proposed filters with other filters in removal impulses noise

The second Experiment is conducted to gauge the efficiency of the proposed technique for filtering images corrupted at different noise ratio. The result of sample image is shown in Figure (4), where the noise ratios for Gaussian noise range from 2.5% to 50%. It is seen visually from these graphical figures that circular averaging filter provides superior results to the other filters in reducing Gaussian at different variance.

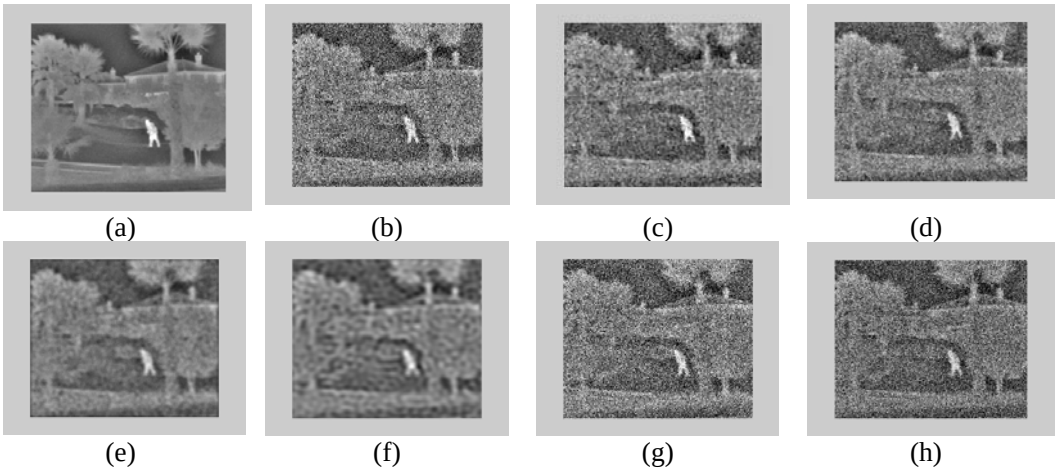

Fig.4. An example of thermal images corrupted by Gaussian noise with variance 5% after applying different filters for noise reduction.(a) Original image, (b) image corrupted with Gaussian noise, (c) applying Median filter, (d) applying Wiener filter, (e) applying circular averaging filter, (f) applying ILP filter, (g) applying BLP filter, (h) applying GLP filter.

To assess the effectiveness of the implemented filters in processing different images. Tables [4, 5, and 6] present the comparison results for images degraded by Gaussian noise. It is seen from these tables that PSNR values of the circular averaging filter has the largest value compared with other filters. So, the circular averaging filter is the most suitable filter for reducing the Gaussian noise. Hence the response of a smoothing linear spatial filter "circular average filter" is simply the average of the pixel contained in the neighborhood of the filter mask, that reduce the effect of the Gaussian noise (linear additive noise).

Table 4. Comparative results in PSNR (dB) of filtering ten different thermal images corrupted by 50% Gaussian noise.

filters	median	wiener	Circular average	ILPF	BLPF	GLPF
Img.1	12.37	18.30	19.68	18.66	9.34	9.28
Img.2	12.06	20.65	21.35	20.57	9.60	9.72
Img.3	11.64	18.21	18.08	17.93	9.58	9.35
Img.4	11.67	18.19	18.45	16.94	9.68	9.71
Img.5	11.61	13.73	14.08	13.45	9.82	9.68
Img.6	11.92	18.92	20.88	18.88	9.67	9.32
Img.7	11.81	18.81	19.82	17.94	9.35	9.66
Img.8	11.79	21.24	22.06	20.56	11.33	10.87
Img.9	12.64	17.68	17.88	16.88	9.64	9.45
Img.10	12.33	18.46	18.55	18.07	9.44	10.16
average	11.98	18.41	19.08	17.98	9.7	9.72

Table 5. Comparative results in PSNR (dB) of filtering ten different thermal images corrupted by 25% Gaussian noise

filters	median	wiener	average	ILPF	BLPF	GLPF
Img.1	16.86	20.27	21.81	20.96	9.90	10.11
Img.2	17.76	21.17	22.75	22.00	9.85	10.76
Img.3	17.26	20.85	19.73	18.76	10.13	10.53
Img.4	17.55	20.11	20.52	20.27	9.56	11.10
Img.5	17.54	15.98	16.56	16.19	10.21	10.54
Img.6	17.35	21.88	22.36	20.65	10.87	10.97
Img.7	17.37	21.40	22.02	20.45	10.43	11.63
Img.8	16.59	22.76	23.87	21.31	9.93	9.98
Img.9	18.22	18.65	19.99	18.25	9.87	9.78
Img.10	17.78	18.94	19.77	20.21	9.61	10.02
average	17.42	20.20	20.93	19.90	10.03	10.54

Table 6. Comparative results in PSNR (dB) of filtering ten different thermal images corrupted by 5% Gaussian noise

filters	median	wiener	average	ILPF	BLPF	GLPF
Img.1	22.10	25.14	26.29	26.71	14.49	14.74
Img.2	20.58	25.00	24.81	25.98	15.65	15.56
Img.3	20.65	23.61	23.90	23.63	15.27	15.35
Img.4	20.56	24.34	24.47	20.51	15.79	15.72
Img.5	20.59	22.76	24.03	23.73	15.36	15.65
Img.6	20.64	24.55	24.34	23.88	15.71	15.33
Img.7	20.69	25.57	26.71	24.66	15.53	15.70
Img.8	19.61	25.23	27.09	25.93	17.00	16.06
Img.9	21.10	23.53	24.39	22.36	15.45	15.38
Img.10	20.78	23.28	21.89	23.79	16.01	15.73
average	20.73	24.30	24.79	24.11	15.62	15.52

Figure (5), Showing the performance comparison of different filters with different variance. It can be shown that PSNR at different values of Gaussian noise variance that, circular average filter has large value comparative with other filters.

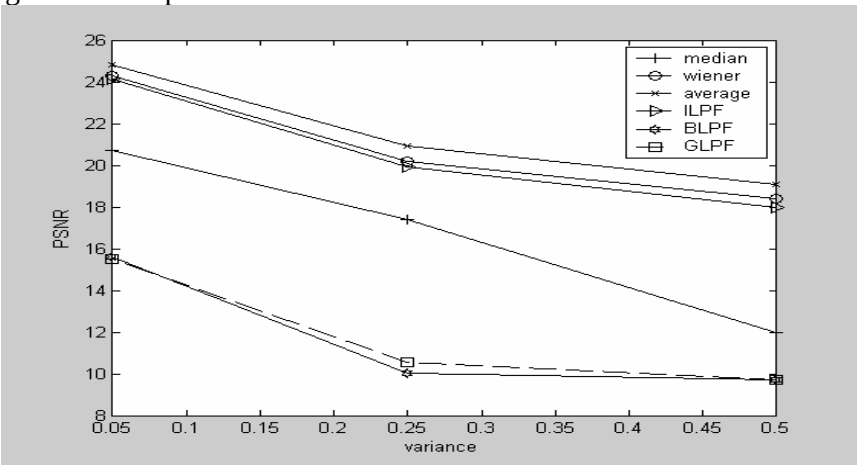

Fig.5. Performance comparison of proposed filters with other filters in removal Gaussian noise.

The third Experiment is conducted to gauge the efficiency of the proposed technique for filtering images corrupted at different noise ratio. The result of sample image is shown in Fig.6, where the noise ratios for speckle noise range from 2.5% to 50%. It is seen visually from these graphical figures that ILPF filter provides superior results to the other filters in reducing speckle noise at different variance.

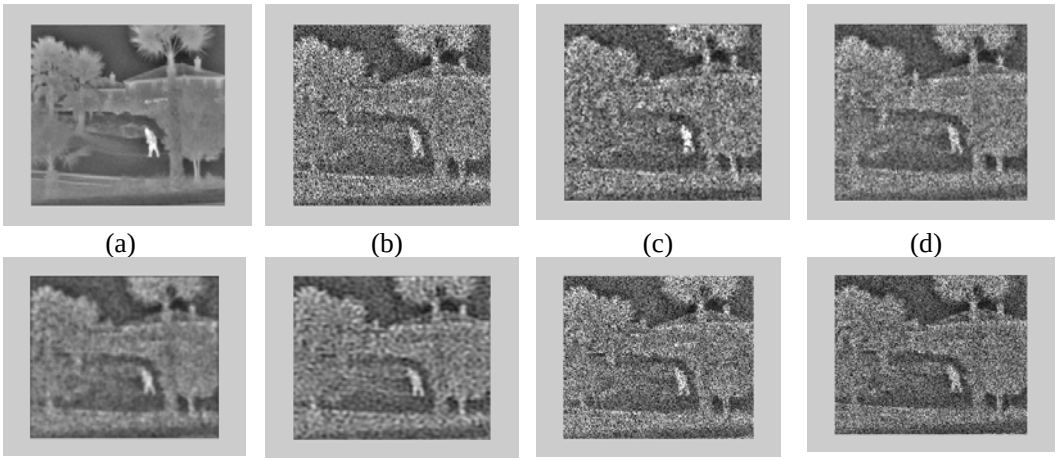

Fig.6. An example of thermal images corrupted by speckle noise with variance 5% after applying different filters for noise reduction.(a) Original image, (b) image corrupted with speckle noise, (c) applying Median filter, (d) applying Wiener filter, (e) applying circular averaging filter, (f) applying ILP filter, (g) applying BLP filter, (h) applying GLP filter.

To assess the effectiveness of the implemented filters in processing different images. Tables [7, 8, and 9] present the comparison results for images degraded by speckle noise. It is seen from these tables that PSNR values of the ILPF filter has the largest value compared with other filters. So, the ILPF filter is the most suitable filter for reducing the speckle noise. Hence it cuts off all frequencies component of the Fourier transform that are at a distance greater than a specified distance from the origin of the transform (attenuate the high frequency component concerned with speckle noise).

Table 7. Comparative results in PSNR (dB) of filtering ten different thermal images corrupted by 50% speckle noise.

filters	median	wiener	average	ILPF	BLPF	GLPF
Img.1	19.61	21.50	24.12	24.93	11.50	12.71
Img.2	20.04	20.32	24.34	25.39	14.22	14.08
Img.3	18.35	21.50	22.61	23.59	10.22	10.00
Img.4	19.32	19.08	21.87	22.51	13.93	14.12
Img.5	15.55	18.72	18.26	19.17	14.01	14.32
Img.6	26.36	22.20	29.20	29.41	10.03	10.26
Img.7	18.16	21.18	22.05	22.99	10.01	9.75
Img.8	20.82	22.13	25.01	26.01	14.57	13.86
Img.9	19.56	23.91	24.09	25.26	10.04	9.24
Img.10	15.41	18.16	17.75	18.61	11.09	10.01
average	19.31	20.87	22.93	23.87	11.96	11.83

Table 8. Comparative results in PSNR (dB) of filtering ten different thermal images corrupted by 25% speckle noise

filters	median	wiener	average	ILPF	BLPF	GLPF
Img.1	22.40	23.44	26.32	27.20	13.28	13.42
Img.2	22.73	22.21	26.46	27.50	13.63	14.54
Img.3	21.09	23.21	24.43	25.40	14.21	13.43
Img.4	22.21	20.99	24.16	25.16	14.32	14.76
Img.5	18.32	22.11	21.09	22.57	14.56	14.83
Img.6	28.43	24.42	30.98	31.20	13.94	14.63
Img.7	20.90	22.77	23.89	25.06	14.52	14.78
Img.8	23.51	24.41	26.96	28.03	14.11	13.75
Img.9	22.44	25.48	26.11	27.40	13.33	13.41
Img.10	18.03	21.42	20.91	22.30	13.06	13.28
average	22.00	23.04	25.13	26.18	13.89	14.08

Table 9. Comparative results in PSNR (dB) of filtering ten different thermal images corrupted by 5% speckle noise

filters	median	wiener	average	ILPF	BLPF	GLPF
Img.1	28.37	29.58	29.08	30.62	21.20	19.89
Img.2	28.70	28.47	29.41	31.01	23.50	22.83
Img.3	26.89	27.97	27.71	28.88	19.56	18.02
Img.4	28.04	27.13	28.07	28.66	23.12	22.44
Img.5	25.09	28.41	25.79	29.76	23.31	23.04
Img.6	32.09	29.93	32.79	32.49	19.44	17.87
Img.7	26.57	27.54	27.20	28.41	19.37	17.44
Img.8	29.43	30.02	29.83	31.23	21.91	20.30
Img.9	28.59	30.76	29.32	31.98	16.99	16.34
Img.10	24.66	28.32	25.73	30.04	19.60	16.57
average	27.84	28.81	28.49	30.30	20.8	19.47

Figure (7), Showing the performance comparison of different filters with different variance of speckle noise. It can be shown that PSNR at different values of speckle noise variance that, ILPF filter has large value comparative with other filters.

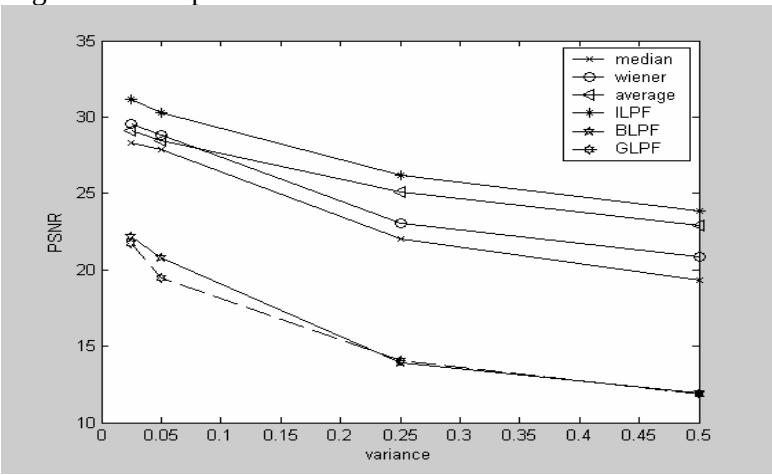

Fig.7. Performance comparison of proposed filters with other filters in removal speckle Noise. The fourth experiment is conducted to gauge the efficiency of the proposed technique for reducing FPN the main dominant noise associated with thermal images. The result of thermal image is shown in Figures (8), (9). It could be noticed from vision observation that NUC algorithm (homomorph filter) for improving the appearance of an image by simultaneous gray-level range compression and contrast enhancement. It has the better performance; hence more details of images were very clearly compared with the original image.

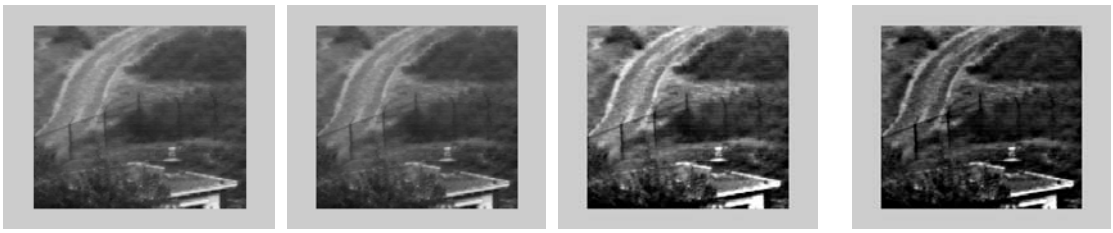

(a) (b) © (d)

Fig.8. An example of thermal images associated with FPN after applying non-uniformity correction algorithm. (a) Original image, (b) Temporal HPF, (c) Homomorph filter at c=10, (d) Homomorph filter at c=2.

Table (10) Showing that the performance of output image depends on the control sharpness constant "c" of the image, Where better performance were found on different thermal images, since we have a higher PSNR at c=10 comparison with other c values.

Table 10. Comparative results in PSNR (dB) of NUC techniques at different degree of brightness (c).

Image	C=2	C=5	C=10	C=12	C=15
1st image	16.25	18.15	**21.34**	20.13	19.54
2nd image	15.90	16.34	**22.83**	21.27	21.02
3rd image	18.71	20.11	**26.35**	22.14	23.16
4th image	14.79	15.67	**20.49**	20.01	19.87

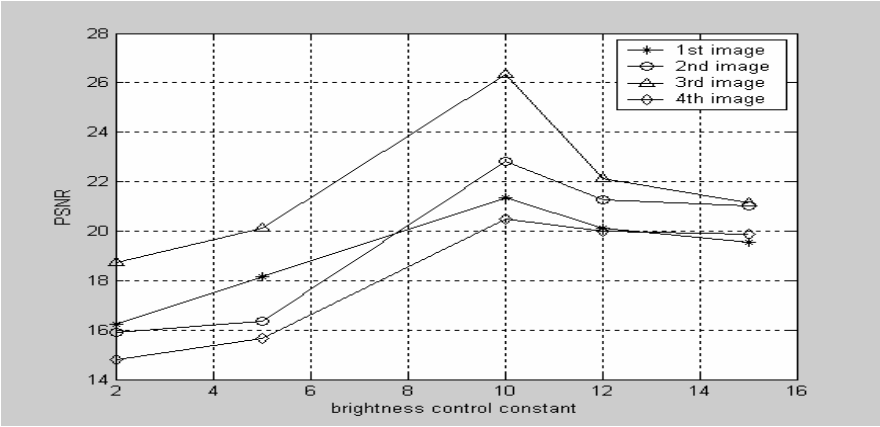

Fig.9. Performance comparison of proposed techniques using control parameters of homomorphic filter

5- Conclusions

This paper introduced most of filters used for improving the performance of thermal images. The experimental results clarified that

- Median filter is considered the most suitable enhancement filter to reduce impulse noises associated with thermal images.
- Circular average filter is considered the most suitable enhancement filter to reduce additive noises associated with thermal images.
- ILPF filter is considered the most suitable enhancement filter to reduce multiplicative noises associated with thermal images.
- Non-uniformity correction (NUC) is the most suitable algorithm to reduce the additive noises represented in FPN which is the main dominant noise affected the performance of thermal images.

References

[1] D. Abhay Sharma, "digital noise", photo techniques magazine, 61-62, Dec. 2001, www.phototechmag.com.

[2] R. I. Hornsey, "part III: noise in image sensor", www.cs.yorku.ca.

[3] Russell C. Hardie, Majeed M. Hayat, Bradley M.Ratliff. And J. Scott Tyo, "an algebraic restoration method for estimating fixed-pattern noise in infrared imagery from a video sequence". Department of electrical and computer engineering, university of New Mexico, Sagalu@ece.unm.edu. 2001.

[4] Torsten Seemann, "digital image processing using local segmentation", Doctor of philosophy, Monash University, Australia, April 2002.

[5] B. R. Corner, R. M Naraynanan, S. E. Reichenbach, " noise estimation in remote sensing imagery using data masking", Int. J. Remote sensing, Vol. 24, No. 4, 689-702, 2003.

[6] Kh. Manglem Singh and Prabin K. Bora, "Adaptive rank-ordered mean filter for removal of impulse noise from images", India, manglem_singh@postmark.net .

[7] E. Abreu, M. Lightstone, S. K. Metra, and K. Arackwa, " anew efficient approach for the removal of impulse noise from highly corrupted image," IEEE Trans. image processing, Vol. 8, No. 6, Jun. 1996.

[8] Guy E.Blelloch, "Introduction to Data Compression ", Guy E.Blelloch, computer science department, Carnegie Mellon University, October 16, 2001.

[9] Rafel C.Gonzalez , Richard E.Woods, "Digital Image Processing", Second edition,university of Tennesse, MedData Interactive, 2002.

[10] Petter Torle, "scene-based correction of image sensor deficiencies", Master's thesis in image processing, Linkopings University, May 6, 2003.